Quantum vector spin glasses with random Dzyaloshinsky-Moriya interactions

T. K. Kopeć* and G. Büttner
Theoretische Tieftemperaturphysik, Universität Duisburg, Lotharstrasse 1, 4100 Duisburg 1, Federal Republic of Germany
(Received 10 December 1990)

The infinite-range quantum vector spin glass with random Dzyaloshinsky-Moriya anisotropy (with variances J and D for random bonds and anisotropy, respectively) and external magnetic field (h) is studied by means of the thermofield dynamics as a substitute for the replica method for the spin values $S=\frac{1}{2}$, 1, and $\frac{3}{2}$. The temperature-anisotropy phase diagrams have been calculated numerically for arbitrary anisotropy and different values of the applied magnetic field h. The stability analysis of the mean-field-type solution against the action of fluctuations has been performed, leading to the upper and lower critical lines in the field-temperature plane. For small values of the reduced anisotropy variance $d=D/J$ ($0.1<d<0.3$), we find a crossover of the upper critical line from the de Almeida–Thouless (AT) -type behavior [$T_c(h)\propto h^{2/3}$] for small fields to the Gabay-Toulouse (GT) -like behavior [$T_c(h)\propto h^2$] for large fields. For larger anisotropies ($d\geq 0.3$) the upper critical line is essentially that of the AT type. Interestingly, the lower critical line, which persists for $d<0.5$, exhibits the reverse type of behavior for the corresponding values of the anisotropy d. Additionally, we have analyzed transverse and longitudinal susceptibilities for different values of the field h. We found that a small amount of the anisotropy d stabilizes a plateau of the local susceptibilities in the spin-glass phase.

I. INTRODUCTION

In recent years it has been found that many of the spin-glass properties are strongly influenced by various types of anisotropies. Specifically, a pronounced anisotropy influence has been found in a number of hexagonal metallic spin-glass systems,[1–3] which behave either Ising-like or Heisenberg-like, depending on the sign and size of the single-spin uniaxial anisotropy energy. Theoretically, uniaxial anisotropy brings about several new features which have been investigated either in classical[4–6] or quantum-spin-glass models.[7–11] In particular, it has been shown that the corresponding problem in the quantum limit behaves qualitatively distinct from its classical counterpart. As has been demonstrated,[9,10] for a large negative uniaxial anisotropy and integer-valued quantum spins, one expects a condensation in the $S_z=0$ state resulting in a nonmagnetic spin state accompanied by the destruction of the spin-glass phase. Therefore, the investigation of various anisotropic agencies in spin glasses constitutes a subject of current interest.

Experiments on the canonical spin glasses as *Cu*Mn and *Ag*Mn in the presence of non-magnetic impurities (e.g., Au or Pt) with strong spin-orbit coupling to the conduction electrons[12] reveal the existence of an anisotropy which is associated with the direction of the remanent magnetization, but not connected with any crystallographic direction.[13] It turns out that this kind of anisotropy can be explained by the Dzyaloshinsky-Moriya (DM) interaction[14] which describes the scattering of the conduction electrons of the host (Cu) by Mn spins via the spin-orbit exchange of the nonmagnetic impurity. Theoretically the influence of the DM interaction has been investigated in Monte Carlo simulations for classical spin-glass systems[15] as well as in analytical studies with random DM exchange.[16–18] It has been found that random DM is expected to play an important role in the spin-glass transition, in particular, in the presence of an applied magnetic field. Qualitative studies performed with classical spins[16] and small anisotropies indicate the appearance of interesting crossovers between Ising- and Heisenberg-like behavior for certain ranges of anisotropy and applied fields.

In the present paper we investigate in detail the quantitative properties of a Heisenberg model with both random Dzyaloshinsky-Moriya anisotropy (of arbitrary value) and applied external magnetic field with special emphasis on the crossover effects. Moreover, we consider the (more realistic) quantum limit and analyze several distinct cases corresponding to the spin dimensionalities $S=\frac{1}{2}$, 1, and $\frac{3}{2}$, which might be of interest from an experimental point of view.

As emphasized elsewhere, the quantum spin glass in comparison with its classical counterpart is far from being a trivial one due to the noncommutativity of the operators involved which require special methods to handle it.[19–23] Typically, quantum mechanics manifests itself via time-dependent self-interactions and order parameters and, in contrast to the classical spin-glass systems, the dynamics becomes an inherent feature of the problem which significantly influences the calculation of e.g., critical lines and transition points. The technique employed here to deal with both randomness and quantum features was introduced by one of us[24] and has successfully been implemented to other quantum-spin-glass problems.[21–23,25] It is based on the thermofield dynamics

method[26] (TFD), which presents a real-time finite-temperature quantum-field theory. Apart from intrinsic interest in dynamics, this method allows one to avoid the use of the n-replica trick, simultaneously dealing with the physical observables like response and correlation functions. In this respect, the TFD method can be regarded as a quantum counterpart of the Martin-Rose-Siggia[27] formalism, known as the dynamic approach to classical spin-glass problems (see, e.g., Ref. 28).

In the following we will present calculations of the anisotropy-temperature phase diagrams for several values of quantum spins including the influence of an applied magnetic field. Phase-transition points and lines are found separating nonergodic spin-glass phases as indicated by the corresponding stability analysis. Special attention will be paid to the study of the variety of crossovers from the Ising-like longitudinal freezing to the Heisenberg-like behavior in the field-temperature plane as manifested by explicit numerical calculation of upper and lower instability lines for arbitrary values of the random anisotropy. Specifically, we establish the range of thermodynamic parameter involved for their occurrence. Furthermore, we evaluate anisotropy, field, and temperature dependence of longitudinal and transverse susceptibilities as well as the corresponding spin-glass order parameters which might be of interest while comparing the predictions of the present work with experiments.

II. PRELIMINARIES

To facilitate the construction of the mean-field theory for the present problem, we adopt a Hamiltonian

$$H=-\sum_{i,j=1}^{N}[J_{ij}\mathbf{S}_i\cdot\mathbf{S}_j+\mathbf{D}_{ij}\cdot(\mathbf{S}_i\times\mathbf{S}_j)]+\sum_{i=1}^{N}H_{0i}\ , \tag{1}$$

which describes the interaction of the quantum spins associated with the local moment S via the set exchanges $\{J_{ij}\}$ and $\{\mathbf{D}_{ij}=(D^x,D^y,D^z)_{ij}\}$, the latter corresponding to the DM interaction. Here, the spin vector $\mathbf{S}=(S_x,S_y,S_z)$ at a given site obeys the familiar spin algebra commutation relation

$$[S_\mu,S_\nu]_-=i\sum_\alpha\epsilon_{\mu\nu\alpha}S_\alpha \tag{2}$$

and the multiplicity S is defined by

$$\prod_{l=0}^{2S}(S_\mu+S-l)=0 \tag{3}$$

with $\mu=x,y,z$ and $\mathbf{S}\cdot\mathbf{S}=S(S+1)$. The $J_{ij}(i\neq j)$ are quenched, independently distributed exchange interactions with the probability distribution

$$P(J_{ij})=(N/2\pi J^2)^{1/2}\exp(-NJ_{ij}^2/2J^2)\ . \tag{4}$$

A similar distribution is assumed for the anisotropy constants

$$P(\mathbf{D}_{ij})=(N/2\pi D^2)^{3/2}\exp[-N(\mathbf{D}_{ij}\cdot\mathbf{D}_{ij})/2D^2]\ . \tag{5}$$

As usual, the scaling of the variances J/N and D/N ensures a sensible thermodynamic limit $N\to\infty$. The second term in Eq. (1) is given by

$$H_{0i}=-hS_{zi} \tag{6}$$

and describes the action of the magnetic field along the z direction.

To proceed within the TFD approach, we recall the correspondence between the conventional statistical average and the TFD expectation value[26] for a given operator A:

$$\langle O(\beta)|A|O(\beta)\rangle=\mathrm{Tr}(e^{-\beta H}A)/\mathrm{Tr}(e^{-\beta H})\ . \tag{7}$$

Here, the temperature-dependent vacuum is introduced where $\beta=1/k_BT$ with k_B being the Boltzmann constant and T the temperature, while H represents the Hamiltonian of the system. In order to have a consistent operator formalism, one needs to double the operator degrees of freedom. Corresponding to any operator A, a tilde operator $\tilde{A}$ is introduced. There is a mapping between A and $\tilde{A}$ called the tilde conjugation rules,[26] equivalent to the Kubo-Martin-Schwinger condition.[26] By using two equivalent operator sets $\{A\}$ and $\{\tilde{A}\}$, the thermal vacuum is expressed as

$$|O(\beta)\rangle=\sum_n e^{-\beta E_n/2}|n\tilde{n}\rangle Z^{-1/2}(\beta)\ , \tag{8}$$

where $|n\rangle$ and $|\tilde{n}\rangle$ are the eigenstates (with the eigenenergies E_n) of the Hamiltonians H and $\tilde{H}$, respectively, and $Z(\beta)=\mathrm{Tr}\exp(-\beta H)$. Correspondingly, many properties of the usual quantum-field theory can be extended to finite-temperatures provided that one works with the total thermal Hamiltonian

$$\hat{H}=H-\tilde{H} \tag{9}$$

rather than with H alone. The best merit of the TFD method when applied to the quantum disordered systems lies in the fact that, due to the vacuum normalization condition[29] $\langle O(\beta)|O(\beta)\rangle=1$, one avoids the so-called "denominator problem" obstructing the calculation of the quenched average and forcing one to use the n-replica trick.

III. QUENCHED AVERAGE AND FUNCTIONAL INTEGRAL FORMULATION

As usual, in the dynamic approach we shall discuss the thermodynamics of the system in terms of the disorder averaged generating functional for the TFD causal Green's functions

$$\langle Z[\eta]\rangle_{J,D}=\int\prod_{i,j}\prod_\mu dJ_{ij}dD_{ij}^\mu P(J_{ij})P(D_{ij}^\mu)Z[\eta,\{J_{ij}\},\{\mathbf{D}_{ij}\}]\ , \tag{10}$$

where $Z[\eta,\{J_{ij}\},\{\mathbf{D}_{ij}\}]$ is the unaveraged generating functional for a fixed realization of random bonds and $\langle\cdots\rangle_{J,D}$ represents the subsequent average with respect to the probability distribution (4,5). Specifically, in the interaction picture with respect to the single-body Hamiltonian (6), one obtains the unaveraged generating functional

$$Z[\eta,\{J_{ij}\},\{\mathbf{D}_{ij}\}]=\left\langle O,\beta\left|T_t\exp\left[-i\int_{-\infty}^{+\infty}dt[\hat{H}_I(t)+\Lambda_\eta(t)]\right]\right|O,\beta\right\rangle , \tag{11}$$

where $|O,\beta\rangle$ refers to the thermal vacuum corresponding to the single-site Hamiltonian (6) while

$$\hat{H}_I(t)=\sum_a \epsilon_a\{J_{ij}\mathbf{S}_i^a(t)\cdot\mathbf{S}_j^a(t)+\mathbf{D}_{ij}[\mathbf{S}_i^a(t)\times\mathbf{S}_j^a(t)]\} \tag{12}$$

and

$$\Lambda_\eta(t)=\int_{-\infty}^{+\infty}dt'\Lambda_\eta(t,t') , \tag{13}$$

where

$$\Lambda_\eta(t,t')=\frac{1}{N}\sum_i\sum_{a,b}\sum_{\mu,\nu}(\epsilon_a\epsilon_b)^{1/2}\eta_{\mu\nu}^{ab}(t,t')S_{\mu i}^a(t)S_{\nu i}^b(t') \tag{14}$$

represents the source term to account for the nonlocal (in time) expectation values of the composite spin operators. Furthermore, $\epsilon_1=1$, $\epsilon_2=-1$, and the spin operators are defined in the interaction picture in the standard way as

$$S_{\mu i}^a(t)=\exp(i\hat{H}_0t)S_{\mu i}^a\exp(-i\hat{H}_0t) , \tag{15}$$

where $\mu=x,y,z$ and the thermodoublet notation has been adopted $S_\mu^1=S_\mu$, $S_\mu^2=\tilde{S}_\mu$. The disorder average (10) amounts in a Gaussian integration over J_{ij} and $\mathbf{D}_{ij}$ variables

$$\langle Z[\eta]\rangle_{J,D}=\left\langle O,\beta\left|T_t\exp\left[-\int_{-\infty}^{+\infty}dt\int_{-\infty}^{+\infty}dt'[\hat{K}(t,t')+\Lambda_\eta(t,t')]\right]\right|O,\beta\right\rangle , \tag{16}$$

where the effective four-spin coupling reads

$$\hat{K}(t,t')=\frac{1}{2N}\sum_{i\neq j}\sum_{a,b}\epsilon_a\epsilon_b\{J^2[\mathbf{S}_i^a(t)\cdot\mathbf{S}_j^a(t)][\mathbf{S}_i^b(t')\cdot\mathbf{S}_j^b(t')]+D^2[\mathbf{S}_i^a(t)\times\mathbf{S}_j^a(t)]\cdot[\mathbf{S}_i^b(t')\times\mathbf{S}_j^b(t')]\} . \tag{17}$$

Now, using the vector identity

$$(\mathbf{A}\times\mathbf{B})\cdot(\mathbf{C}\times\mathbf{D})=(\mathbf{A}\cdot\mathbf{C})(\mathbf{B}\cdot\mathbf{D})-(\mathbf{B}\cdot\mathbf{C})(\mathbf{A}\cdot\mathbf{D}) , \tag{18}$$

one obtains, after some algebra,

$$\hat{K}(t,t')=\frac{1}{2N}\sum_{i\neq j}\sum_{a,b}\epsilon_a\epsilon_b\sum_{\mu,\nu}\{J^2S_{i\mu}^a(t)S_{j\mu}^a(t)S_{i\nu}^b(t')S_{j\nu}^b(t')+D^2[S_{i\mu}^a(t)S_{i\mu}^b(t')S_{j\nu}^a(t)S_{j\nu}^b(t')-S_{j\mu}^a(t)S_{i\mu}^b(t')S_{i\nu}^b(t)S_{j\nu}^a(t')]\} . \tag{19}$$

Subsequently, in the large-N limit, by employing the relation

$$\frac{1}{N}\sum_{i\neq j}A_iA_j=\frac{1}{2N}\left[\sum_i A_i\right]^2+O(1) , \tag{20}$$

we can write the quantity $\hat{K}(t,t')$ as

$$\hat{K}(t,t')=\frac{J^2}{4N}\sum_{a,b}\epsilon_a\epsilon_b\left[(1-d^2)\sum_{\mu,\nu}\left[\sum_i S_{\mu i}^a(t)S_{\nu i}^b(t')\right]^2+d^2\left[\sum_i\sum_\mu S_{\mu i}^a(t)S_{\mu i}^b(t')\right]^2\right]+O(1) . \tag{21}$$

Furthermore, parametrizing according to Sherrington and Kirkpatrick[30] with the help of the Gaussian functional integration, we find, for the averaged generating functional for the causal TFD functions,

$$\langle Z[\eta,\{J_{ij}\},\{\mathbf{D}_{ij}\}]\rangle_{J,D}=\int\prod_{a,b}\prod_{\mu,\nu}DQ_{\mu\nu}^{ab}DR^{ab}\exp(-NL[\mathsf{Q},\mathsf{R}]+\Omega[\eta]) , \tag{22}$$

where the single-site dynamic effective Lagrangian reads

$$L[\mathsf{Q}]=\mathrm{Tr}\mathsf{Q}^2+\mathrm{Tr}\mathsf{R}^2-\ln\Phi[\mathsf{Q},\mathsf{R}] \tag{23}$$

with

$$\mathrm{Tr}\mathsf{Q}^2=\int_{-\infty}^{+\infty}dt\int_{-\infty}^{+\infty}dt'\sum_{a,b}\sum_{\mu,\nu}Q_{\mu\nu}^{ab}(t,t')Q_{\nu\mu}^{ba}(t',t) ,$$
$$\mathrm{Tr}\mathsf{R}^2=\int_{-\infty}^{+\infty}dt\int_{-\infty}^{+\infty}dt'\sum_{a,b}R^{ab}(t,t')R^{ba}(t',t) . \tag{24}$$

Here,

$$Q_{\mu\nu}^{ab}(t,t')=Q_{\nu\mu}^{ba}(t',t)$$

and

$$R^{ab}(t,t')=R^{ba}(t',t)$$

represent symmetric tensor fields which are nonlocal in time. Subsequently, the source term is $\Omega[\eta]=\mathrm{Tr}(Q\eta)/J^2$ and

$$\Phi[Q,R]=\langle O,\beta|U_{QR}(-\infty;+\infty)|O,\beta\rangle\ , \tag{25}$$

while, for the evolution operator in the interaction picture, one obtains

$$U_{QR}(-\infty;+\infty)=T_t\exp\left[-i\int_{-\infty}^{+\infty}dt\int_{-\infty}^{+\infty}dt' H_{Q,R}(t,t')\right] \tag{26}$$

containing the time-ordered exponential resulting from the interaction picture. Furthermore, the effective time-dependent single-site thermal Hamiltonian takes the form

$$\hat{H}_{Q,R}(t,t')=-J\sum_{a,b}\sum_{\mu,\nu}(\epsilon_a\epsilon_b)^{1/2}[(1-d^2)^{1/2}Q^{ab}_{\mu\nu}(t,t')+dR^{ab}(t,t')\delta_{\mu\nu}]S^a_\mu(t)S^b_\nu(t')\ . \tag{27}$$

From Eq. (27) it can be read off that the quantum generalization of the problem results in a time-dependent self-interaction $JQ^{ab}_{\mu\nu}(t,t')$ and $R^{ab}(t,t')$ between spin operators at the same site which have to be determined self-consistently.

In the $N\to\infty$ limit, the steepest descent method can be used which amounts in finding the stationary points $Q^{ab}_{0,\mu\nu}$ and $R^{ab}_0(t,t')$ determined by the extremal conditions

$$\frac{\delta L[Q,R]}{\delta Q^{ab}_{\mu\nu}}=0\ ,\qquad \frac{\delta L[Q,R]}{\delta R^{ab}}=0\ . \tag{28}$$

Thus, one obtains

$$Q^{ab}_{0,\mu\nu}(t,t')=\tfrac{1}{2}(\epsilon_a\epsilon_b)^{1/2}J(1-d^2)^{1/2}G^{ab}_{\mu\nu}(t,t') \tag{29}$$

and, correspondingly,

$$R^{ab}_0(t,t')=\tfrac{1}{2}(\epsilon_a\epsilon_b)^{1/2}d\sum_\mu G^{ab}_{\mu\mu}(t,t') \tag{30}$$

where the causal TFD function is defined as

$$G^{ab}_{\mu\nu}(t,t')=-i\frac{\langle O,\beta|T_tS^a_\mu(t)S^b_\nu(t')U_{Q_0R_0}(-\infty;+\infty)|O,\beta\rangle}{\langle O,\beta|T_tU_{Q_0R_0}(-\infty;+\infty)|O,\beta\rangle}\ . \tag{31}$$

and the averages at the right-hand side of Eq. (31) are calculated with the effective Hamiltonian containing the self-consistency value of the Q and R fields

IV. ORDER PARAMETERS AND SUSCEPTIBILITIES

The location of the spin-glass transition can be described by the divergence of the inverse relaxation rate characterized by a generalized damping function $\Gamma_\mu(\omega)$ ($\mu=x,y,z$), defined as

$$\Gamma^{-1}_\mu(\omega)=i\frac{\partial}{\partial\omega}[G_R^{-1}(\omega)]_{\mu\mu} \tag{32}$$

for $\omega\to 0$ if one approaches the spin-glass freezing temperature from above. Furthermore, by using the Dyson equation for the TFD causal Green's function in the matrix form,

$$\underline{\hat{G}}(\omega)=\hat{\Sigma}(\omega)\frac{1}{1-J\underline{X}(\omega)\hat{\Sigma}(\omega)}\ . \tag{33}$$

The self-energy part and causal TFD Green's function in thermofield space can be diagonalized with the help of the thermal Bogoliubov transformation. For example, the self-energy part [and similarly $\underline{\hat{G}}(\omega)$] can be decomposed as follows:

$$\hat{\Sigma}^{ab}_{\mu\nu}(\omega)=[\underline{U}_B(\omega)\tau\overline{\Sigma}_{\mu\nu}(\omega)\underline{U}_B(\omega)]^{ab} \tag{34}$$

with

$$\underline{U}_B(\omega)=\begin{bmatrix}\sinh\phi(\omega) & \cosh\phi(\omega)\\ \cosh\phi(\omega) & \sinh\phi(\omega)\end{bmatrix},\qquad \sinh^2\phi(\omega)=\frac{1}{e^{\beta\omega}-1} \tag{35}$$

as the thermal transformation matrix.[26] The corresponding diagonal matrices in the thermofield component space are

$$\overline{\Sigma}^{ab}(\omega)=\begin{bmatrix}\Sigma^R_{\mu\nu}(\omega) & 0\\ 0 & \Sigma^A_{\mu\nu}(\omega)\end{bmatrix}^{ab} \tag{36}$$

and

$$\overline{G}^{ab}_{\mu\nu}(\omega)=\begin{bmatrix}G^R_{\mu\nu}(\omega) & 0\\ 0 & G^A_{\mu\nu}(\omega)\end{bmatrix}^{ab},\qquad \tau=\begin{bmatrix}1 & 0\\ 0 & -1\end{bmatrix} \tag{37}$$

with $G^{R(A)}_{\mu\nu}(\omega)$ being the matrix of retarded (advanced) Green's functions. The dynamic spin self-interaction can be written as follows:

$$X^{ab}_{\mu\nu}(\omega)=J\epsilon_a\epsilon_b(1+2d^2)G^{ab}_{\mu\nu}(\omega)\ . \tag{38}$$

Making use of Eqs. (32)–(38) and observing that, in zero field, one has rotational symmetry in the spin-component space

$$[G^{R(A)}_{\mu\nu}(\omega)=G^{R(A)}(\omega)\delta_{\mu\nu},\Sigma^{R(A)}_{\mu\nu}(\omega)=\Sigma^{R(A)}(\omega)\delta_{\mu\nu}]\ ,$$

one can write the Dyson equation in terms of the retarded (advanced) response function, e.g.,

$$\underline{G}^R(\omega)=\frac{\Sigma_R(\omega)}{1-J^2(1+2d^2)\underline{G}^R(\omega)} \tag{39}$$

and, consequently, from Eq. (32)

$$\Gamma^{-1}(\omega)=\frac{G_R^2(\omega)\Sigma_R^{-2}(\omega)}{1-J^2(1+2d^2)G_R^2(\omega)}\frac{\partial\Sigma_R(\omega)}{\partial\omega} . \tag{40}$$

The denominator of Eq. (40) represents the renormalization of the damping function due to the random exchange while the nominator containing the derivative of the self-energy is the further renormalization due to the dynamic self-coupling. We shall assume that $\partial\Sigma_R(\omega)/\partial\omega$ is finite and discuss the resulting low-frequency behavior. In the limit $\omega\rightarrow 0$, Eq. (40) implies a singularity of the inverse relaxation time at the transition temperature T_c. For the zero of the external magnetic field, one obtains

$$k_B T_c(h=0)=\tfrac{1}{3}JS(S+1)(1+2d^2)^{1/2} . \tag{41}$$

Below the freezing temperature in zero field, the onset of the glassy phase is marked by a nonzero value of the spin-glass order parameter. Within the context of the dynamic theory, the spin-glass order parameter has to be determined via time-persistent quantities. To accomplish it, we factorize the matrix of the causal TFD Green's functions into finite-time $(G_{\rm reg})^{ab}_{\mu\nu}$ and time-persistent parts $(G_{\rm sing})^{ab}_{\mu\nu}$ as follows:

$$G^{ab}_{\mu\nu}(t,t')=(G_{\rm reg})^{ab}_{\mu\nu}(t,t')+(G_{\rm sing})^{ab}_{\mu\nu} , \tag{42}$$

where

$$(G_{\rm sing})^{ab}_{\mu\nu}=\lim_{|t-t'|\rightarrow\infty} G^{ab}_{\mu\nu}(t,t') . \tag{43}$$

For the finite-time part, one has restored time-translational invariance in thermal equilibrium

$$G_{\rm reg}(t,t')=G_{\rm reg}(t-t')$$

and the correspondence with measurable quantities is achieved by the following decomposition of the Fourier-transformed causal Green's function in the space of the thermofield components

$$\begin{aligned}(G_{\rm reg})^{ab}_{\mu\nu}(\omega)&=[\underline{U}_B(\omega)\tau\bar{G}_{\mu\nu}(\omega)\underline{U}_B(\omega)]^{ab}\\&=[\tau\bar{G}_{\mu\nu}(\omega)]^{ab}-\frac{2i(C_{\rm reg})_{\mu\nu}(\omega)}{e^{\beta\omega}+1}\begin{bmatrix}1 & e^{\beta\omega/2}\\ e^{\beta\omega/2} & 1\end{bmatrix} .\end{aligned} \tag{44}$$

Here, $(C_{\rm reg})_{\mu\nu}(\omega)$ refers to the matrix of the thermodynamic correlation functions in the spin-component space being related to $G^R_{\mu\nu}(\omega)$ by means of the usual fluctuation-dissipation theorem. Furthermore, it turns out that the time-persistent part $(G_{\rm sing})^{ab}_{\mu\nu}(\omega)$ has the form

$$(G_{\rm sing})^{ab}_{\mu\nu}(\omega)=-2\pi i q_{\mu\mu}\delta_{\mu\nu}\delta(\omega)\begin{bmatrix}1 & 1\\ 1 & 1\end{bmatrix}^{ab} , \tag{45}$$

where

$$q_{\mu\nu}=q_L\delta_{\mu z}+q_T(1-\delta_{\mu z}) \tag{46}$$

is the Edwards-Anderson (EA) spin-glass order parameter[31] and q_L and q_T are the order parameters associated with longitudinal and transverse spin-glass ordering, respectively. In fact, by substituting Eq. (45) into (44) and using (42), one obtains, for the total correlation function,

$$C_{\mu\nu}(\omega)=(C_{\rm reg})_{\mu\nu}(\omega)+2\pi q_{\mu\nu}\delta(\omega) \tag{47}$$

in accordance with the standard dynamic definition of the EA spin-glass order parameter.

Because of the appearance of the dynamic self-interaction $JQ^{ab}_{\mu\nu}(\omega)$ in the effective thermal Hamiltonian (27), the explicit solution of Eq. (31) is a rather formidable task. For this reason we will focus on the effects of quantum fluctuations on a time scale such that the finite-time part of the dynamic self-interaction can be presented by an instantaneous term

$$(Q_{\rm reg})^{ab}_{\mu\nu}(t-t')=\tfrac{1}{2}(\epsilon_a\epsilon_b)^{1/2}J\chi_{\mu\nu}\delta(t-t')\delta_{ab} , \tag{48}$$

where

$$\chi_{\mu\nu}=\lim_{\omega\rightarrow 0}G^R_{\mu\nu}(\omega)=\lim_{\omega\rightarrow 0}G^A_{\mu\nu}(\omega) \tag{49}$$

is the matrix of static susceptibilities which can be decomposed into longitudinal and transverse parts according to

$$\chi_{\mu\nu}=\delta_{\mu\nu}[\chi_L\delta_{\mu z}+\chi_T(1-\delta_{\mu z})] . \tag{50}$$

The time-persistent contribution to the effective thermal Hamiltonian can be represented by using auxiliary Gaussian integrations having the form of a static Gaussian noise which acts as a random field to generate time-persistent autocorrelations. Accordingly, the self-consistent equation (31) becomes

$$G^{ab}_{\mu\nu}(t-t')=\langle G^{ab}_{\mu\nu}(t-t'|\mathbf{z})\rangle_z , \tag{51}$$

where, for the noise-dependent unaveraged causal Green's functions with the use of the vacuum normalization condition we get

$$G^{ab}_{\mu\nu}(t-t'|\mathbf{z})=-i\langle O(\beta,\mathbf{z})|T_t S^a_\mu(t)S^b_\nu(t')U_{Q_0R_0}(-\infty;+\infty|\mathbf{z})|O(\beta,\mathbf{z})\rangle \tag{52}$$

with

$$U_{Q_0R_0}(-\infty;+\infty|\mathbf{z})=T_t\exp\left[-i\int_{-\infty}^{+\infty}dt\,\hat{H}(t|\mathbf{z})\right] \quad (53)$$

and the Gaussian average over the static noise $\mathbf{z}=(z_x,z_y,z_z)$ is given by

$$\langle\cdots\rangle_z=\int_{-\infty}^{+\infty}\frac{d^3\mathbf{z}}{(2\pi)^{3/2}}e^{-|\mathbf{z}|^2/2}\cdots . \quad (54)$$

Here, $|O(\beta,\mathbf{z})\rangle$ is the thermal vacuum associated with the single-site effective Hamiltonian

$$H_0'(\mathbf{z})=H_0-\sum_\mu J\left[(1-d^2)q_{\mu\mu}+d^2\left[\sum_\nu q_{\nu\nu}\right]\right]^{1/2}z_\mu S_\mu , \quad (55)$$

which contains the static noise, while the time-ordered exponential contains only the finite-time part of the dynamic self-interaction. The corresponding total single-site effective Hamiltonian can be then established via the correspondence (7)–(9) with its thermal counterpart and reads

$$H(\mathbf{z})=-\tfrac{1}{2}J^2\left[(1-d^2)\sum_{\mu,\nu}\chi_{\mu\nu}S_\mu S_\nu+d^2\sum_\mu\chi_{\mu\mu}\sum_\nu(S_\nu)^2\right]+H_0'(\mathbf{z}) . \quad (56)$$

From Eq. (56) it is seen that various susceptibilities couple to the squares of spin operators and thus $\chi_{\mu\nu}$ can be considered as a kind of quadrupolar order parameter which should be determined self-consistently together with $q_{\mu\mu}$. The corresponding self-consistency equations which follow from Eqs. (43) and (49)–(56) are then

$$q_\mu=\langle m_\mu^2(\mathbf{z})\rangle_z,\quad \chi_{\mu\nu}=\langle\chi_{\mu\nu}(\mathbf{z})\rangle_z , \quad (57)$$

where $\mu,\nu=x,y,z$, while $m_\mu(\mathbf{z})$ and

$$\chi_{\mu\nu}(\mathbf{z})=G^R_{\mu\nu}(\omega=0,\mathbf{z})$$

are the magnetization induced by the static random fields and the unaveraged susceptibility, respectively. Furthermore,

$$m_\mu(\mathbf{z})=-\sum_{l=0}^{2S}[\partial_\mu\lambda_l(\mathbf{z})]\rho_l(\mathbf{z}) , \quad (58)$$

while

$$\chi_{\mu\nu}(\mathbf{z})=-\sum_{l=0}^{2S}[\partial_\mu\partial_\nu\lambda_l(\mathbf{z})]\rho_l(\mathbf{z})+\beta\left[\sum_{l=0}^{2S}[\partial_\mu\lambda_l(\mathbf{z})][\partial_\nu\lambda_l(\mathbf{z})]\rho_l(\mathbf{z})-m_\mu(\mathbf{z})m_\nu(\mathbf{z})\right] , \quad (59)$$

where

$$\rho_l(\mathbf{z})=\frac{\exp[-\beta\lambda_l(\mathbf{z})]}{\sum_{k=0}^{2S}\exp[-\beta\lambda_k(\mathbf{z})]} . \quad (60)$$

Here, $\lambda_l(\mathbf{z})$ $(l=0,\ldots,2S)$ represents one of the $2S+1$ eigenvalues of the effective single-site quantum-spin Hamiltonian (36), while

$$\partial_\mu\lambda_l(\mathbf{z})\equiv\left[\frac{\partial\lambda_l(\mathbf{z})}{\partial h_\mu}\right]_{h_\mu=0} , \quad (61)$$

where h_μ denotes an infinitesimal longitudinal (transverse) applied magnetic field.

The temperature and field dependences of various suceptibilities and spin-glass order parameters for different anisotropies and quantum-spin numbers are presented in Figs. 1–4. The remarkable feature of the zero-field susceptibilities is that their temperature dependence in the paramagnetic phase is the same irrespective of the aniostropy value. More interesting behavior appears in an applied magnetic field h, where the susceptibilities in the spin-glass phase exhibit a rather weak temperature dependence with increasing anisotropy constant d and a remarkable similarity of the transverse (χ_T) and longitudinal (χ_L) components. This can be explained as a result of the mixing of various modes via the random DM interaction. Indeed, as follows from Eq. (56), the temperature behavior in the paramagnetic phase is determined via the self-consistent solution for the quadrupolar parameters $\chi_{\mu\nu}$. However, for zero field, mixed modes disappear as a result of isotropy and with $\chi_{\mu\nu}=\chi\delta_{\mu\nu}$ and

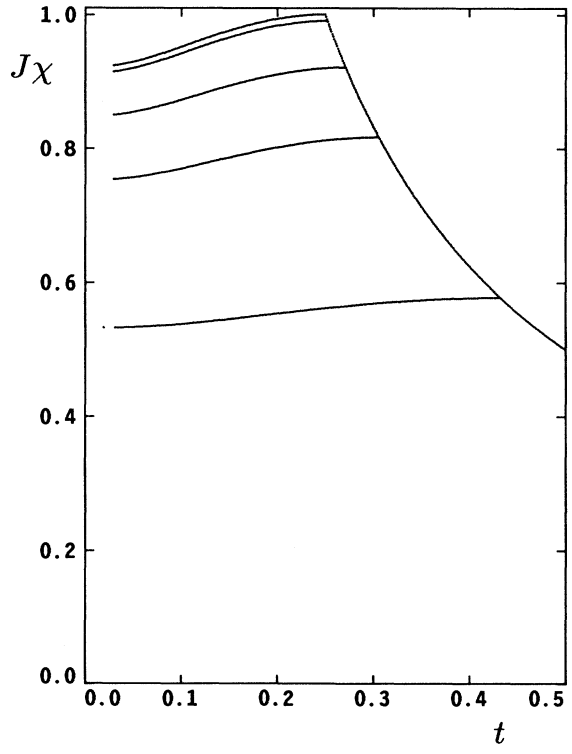

FIG. 1. The temperature ($t=k_BT/J$) dependence of the local static susceptibility for $h=0$ ($\chi=\chi_L=\chi_T$) and $d=0$, 0.1, 0.3, 0.5, 1 (from the top to the bottom, respectively), and for $S=\frac{1}{2}$

the property $\mathbf{S}\cdot\mathbf{S}=S(S+1)$ one arrives at the purely diagonal effective quantum Hamiltonian (56). As a result, the weighting factors (60) are independent of χ, irrespective of the quantum-spin value, resulting in a Curie behavior of the susceptibility in the paramagnetic phase.

V. INSTABILITY LINES AND PHASE DIAGRAMS

The generalized damping function [Eq. (32)] diverges in the static limit ($\omega\rightarrow 0$) also in the case of the applied magnetic field ($h\neq 0$), where it splits into one longitudinal [$\Gamma_z^{-1}(\omega)\equiv\Gamma_L^{-1}(\omega)$] and two transverse relaxation times

$$\Gamma_x^{-1}(\omega)=\Gamma_y^{-1}(\omega)\equiv\Gamma_T^{-1}(\omega) ,$$

respectively. It is convenient to work with the unaveraged TFD causal correlation functions $G_{\mu\nu}^{ab}(\omega,\mathbf{z})$ which depend on the static noise $\mathbf{z}$ and the corresponding self-energy parts $\Sigma_{\mu\nu}^{ab}(\omega,\mathbf{z})$. Specifically, one has

$$\Gamma_\mu^{-1}(\omega)=\left\langle i\frac{\partial}{\partial\omega}[\underline{G}_R^{-1}(\omega,\mathbf{z})]_{\mu\mu}\right\rangle_z , \tag{62}$$

where the unaveraged TFD causal functions can be decomposed with the help of the thermal transformation matrix as follows:

$$\underline{G}(\omega,\mathbf{z})=\underline{U}_B(\omega)\tau\overline{\underline{G}}(\omega,\mathbf{z})\underline{U}_B(\omega) , \tag{63}$$

where

$$\overline{G}_{\mu\nu}^{ab}(\omega,\mathbf{z})=\begin{bmatrix} G_{\mu\nu}^R(\omega,\mathbf{z}) & 0 \\ 0 & G_{\mu\nu}^A(\omega,\mathbf{z})\end{bmatrix}^{ab} . \tag{64}$$

Furthermore, expanding the corresponding Green's function in powers of the self-interaction $\underline{X}$, one obtains

$$\underline{G}(\omega,\mathbf{z})=\hat{\Sigma}(\omega,\mathbf{z})+\hat{\Sigma}(\omega,\mathbf{z})J\underline{X}(\omega)\hat{\Sigma}(\omega,\mathbf{z}) +\hat{\Sigma}(\omega,\mathbf{z})J\underline{X}(\omega)\hat{\Sigma}(\omega,\mathbf{z})J\underline{X}(\omega)\hat{\Sigma}(\omega,\mathbf{z})+\cdots , \tag{65}$$

where

$$X_{\mu\nu}^{ab}(\omega)=J\epsilon_a\epsilon_b\left[(1-d^2)\underline{G}_{\mu\nu}^{ab}(\omega)+d^2\sum_\mu\underline{G}_{\mu\mu}^{ab}(\omega)\right] \tag{66}$$

and $\underline{G}(\omega)=\langle\underline{G}(\omega,\mathbf{z})\rangle_z$ is the averaged causal TFD Green's function.

The expansion (65) is generated by the following Dyson equation for the function $\underline{G}(\omega,\mathbf{z})$:

$$\underline{G}(\omega\mathbf{z})=\hat{\Sigma}(\omega,\mathbf{z})+\hat{\Sigma}(\omega,\mathbf{z})J\underline{X}(\omega)\underline{G}(\omega,\mathbf{z}) , \tag{67}$$

where

$$\hat{\Sigma}(\omega,\mathbf{z})=\underline{U}_B(\omega)\tau\overline{\Sigma}(\omega,\mathbf{z})\underline{U}_B(\omega) \tag{68}$$

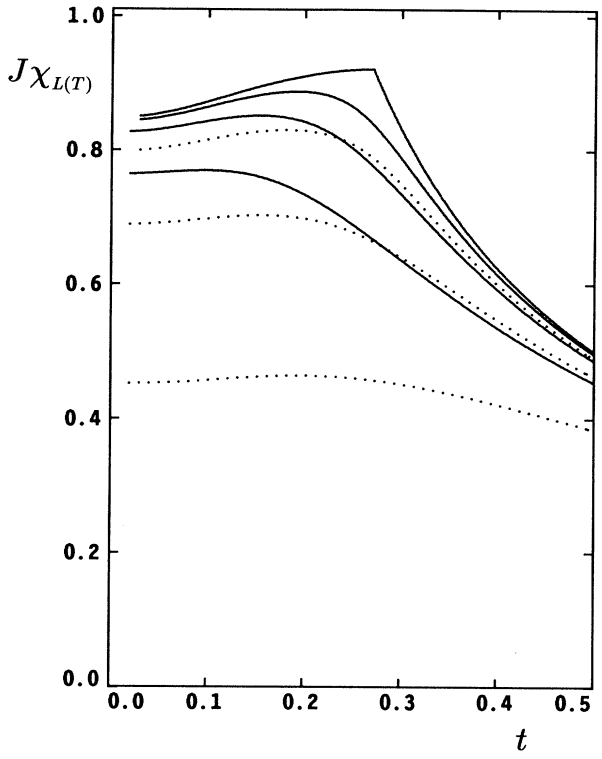

FIG. 2. The temperature ($t=k_BT/J$) dependence of the local static longitudinal (χ_L, dotted lines) and transverse (χ_T, solid lines) susceptibilities for fixed anisotropy $d=0.3$ and different values of the applied field: $h=0$, 0.125, 0.25, 0.5 (from the top to the bottom, respectively). The quantum-spin number is fixed at $S=\frac{1}{2}$.

and

$$\overline{\Sigma}_{\mu\nu}^{ab}(\omega,\mathbf{z})=\begin{bmatrix} \Sigma_{\mu\nu}^R(\omega,\mathbf{z}) & 0 \\ 0 & \Sigma_{\mu\nu}^A(\omega,\mathbf{z})\end{bmatrix}^{ab} . \tag{69}$$

The unaveraged dynamic-response function $\underline{G}^R(\omega,\mathbf{z})$ obeys, in turn, a Dyson equation

$$\underline{G}^R(\omega,\mathbf{z}) =\hat{\Sigma}_R(\omega,\mathbf{z})\{1-J^2[(1-d^2)\underline{G}^R(\omega)+d^2\mathrm{Tr}\underline{G}^R(\omega)]\}^{-1} , \tag{70}$$

which follows directly from the Eqs. (63), (64), and (68)–(70).

Specifically, differentiation of Eq. (71) with respect to the frequency ω leads to

$$\frac{\partial\underline{G}^R(\omega,\mathbf{z})}{\partial\omega}=J^2\left[(1-d^2)\underline{G}^R(\omega,\mathbf{z})\frac{\partial\underline{G}^R(\omega)}{\partial\omega}\underline{G}^R(\omega,\mathbf{z})+d^2\mathrm{Tr}\left[\underline{G}^R(\omega,\mathbf{z})\frac{\partial\underline{G}^R(\omega)}{\partial\omega}\underline{G}^R(\omega,\mathbf{z})\right]\right] +\underline{G}^R(\omega,\mathbf{z})\hat{\Sigma}_R^{-1}(\omega,\mathbf{z})\frac{\partial\hat{\Sigma}_R(\omega,\mathbf{z})}{\partial\omega}\hat{\Sigma}_R^{-1}(\omega,\mathbf{z})\underline{G}^R(\omega,\mathbf{z}) , \tag{71}$$

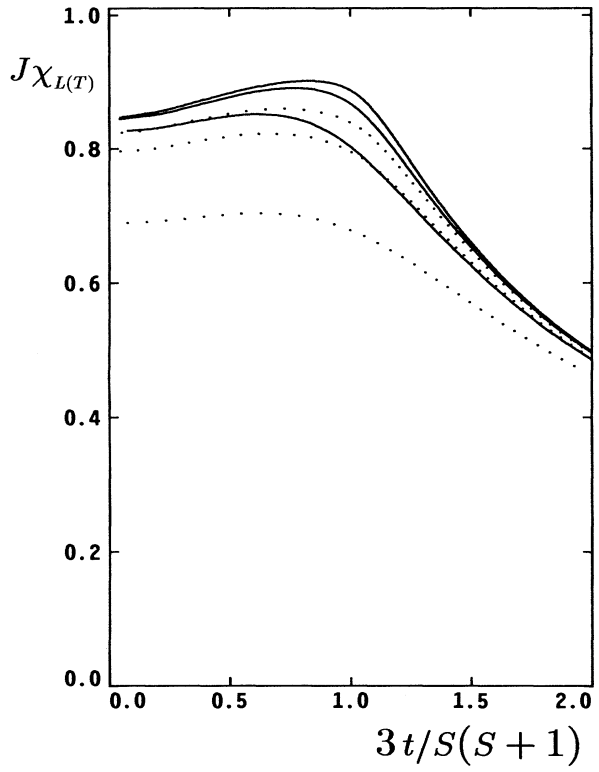

FIG. 3. The temperature ($t=k_BT/J$) dependence of the local static longitudinal (χ_L, dotted lines) and transverse (χ_T, solid lines) susceptibilities for $h=0.25$ and $d=0.3$ for different values of the quantum-spin number: $S=\frac{1}{2}$, 1, $\frac{3}{2}$ (from the bottom to the top, respectively).

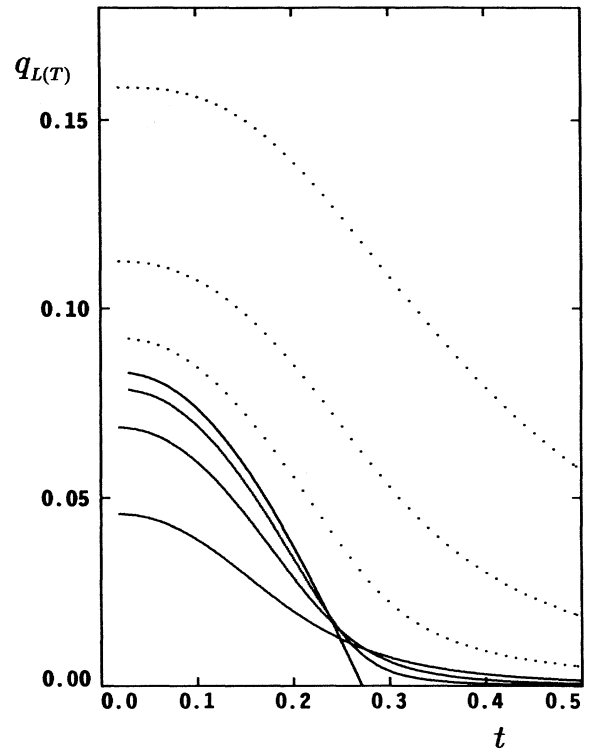

FIG. 4. The temperature ($t=k_BT/J$) dependence of the longitudinal (q_L, dotted lines) and transverse (q_T, solid lines) spin-glass order parameter for fixed anisotropy $d=0.3$ and different values of the applied field: $h=0$, 0.125, 0.25, 0.5 (from the top to the bottom for transverse and from the bottom to the top for longitudinal components, respectively). The $h=0$ curve is identical for q_L and q_T and cut the temperature axis at T_c ($h=0$) [Eq. (41)]. The quantum-spin number is fixed at $S=\frac{1}{2}$.

while, for the static-noise averaged quantities, one has, in terms of spatial components ($\alpha=x,y,z$)

$$\sum_{\nu}\left[\delta_{\mu\nu}-J^2\left[(1-d^2)\chi^{(2)}_{\mu\nu}(\omega)+d^2\sum_{\alpha}\chi^{(2)}_{\mu\alpha}(\omega)\right]\right]\left[\frac{\partial \underline{G}^R(\omega)}{\partial\omega}\right]_{\nu\nu}$$
$$=\sum_{\alpha,\beta,\gamma,\delta}\langle \underline{G}^R_{\mu\alpha}(\omega,\mathbf{z})[\hat{\Sigma}^{-1}_R(\omega,\mathbf{z})]_{\alpha\beta}\left[\frac{\partial\hat{\Sigma}_R(\omega,\mathbf{z})}{\partial\omega}\right]_{\beta\gamma}[\hat{\Sigma}^{-1}_R(\omega,\mathbf{z})]_{\gamma\delta}\underline{G}^R_{\delta\mu}(\omega,\mathbf{z})\rangle_z\ , \tag{72}$$

where we have adopted the notation

$$\chi^{(2)}_{\mu\nu}(\omega)=\langle[\underline{G}^R_{\mu\nu}(\omega,\mathbf{z})]^2\rangle_z\ . \tag{73}$$

Furthermore, by observing the rotational symmetry with respect to the z axis (the direction of applied field), one can explicitly write

$$\chi^{(2)}_{\mu\nu}(\omega)=\begin{bmatrix}\chi^{(2)}_T(\omega) & \chi^{(2)}_{xy}(\omega) & \chi^{(2)}_{xz}(\omega)\\ \chi^{(2)}_{xy}(\omega) & \chi^{(2)}_T(\omega) & \chi^{(2)}_{xz}(\omega)\\ \chi^{(2)}_{xz}(\omega) & \chi^{(2)}_{xz}(\omega) & \chi^{(2)}_L(\omega)\end{bmatrix}\ . \tag{74}$$

The condition for divergence of the inverse generalized damping functions $\Gamma^{-1}_{\mu}(\omega=0)$, which is equivalent to the marginal stability reads $\kappa=0$, where κ belongs to the set of eigenvalues of the matrix $\underline{A}$

$$A_{\mu\nu}=\delta_{\mu\nu}-J^2\left[(1-d^2)\chi^{(2)}_{\mu\nu}(0)+d^2\sum_{\alpha}\chi^{(2)}_{\mu\alpha}(0)\right] \tag{75}$$

determined from the following equation:

$$\det(\underline{A}-\kappa\mathbb{1})=0 \ . \tag{76}$$

Specifically, taking into account Eqs. (75) and (76), one obtains the following components of $\underline{A}$:

$$\underline{A}=\begin{bmatrix} A_{11} & A_{12} & A_{13} \\ A_{12} & A_{11} & A_{13} \\ A_{31} & A_{31} & A_{33} \end{bmatrix} \tag{77}$$

with

$$\begin{aligned} A_{11}&=1-J^2\{\chi_T^{(2)}(0)+d^2[\chi_{xy}^{(2)}(0)+\chi_{xz}^{(2)}(0)]\} \ , \\ A_{12}&=-J^2\{\chi_{xy}^{(2)}(0)+d^2[\chi_T^{(2)}(0)+\chi_{xz}^{(2)}(0)]\} \ , \\ A_{13}&=-J^2\{\chi_{xz}^{(2)}(0)+d^2[\chi_T^{(2)}(0)+\chi_{xy}^{(2)}(0)]\} \ , \\ A_{31}&=-J^2\{\chi_{xz}^{(2)}(0)+d^2[\chi_L^{(2)}(0)+\chi_{xz}^{(2)}(0)]\} \ , \\ A_{33}&=1-J^2[\chi_L^{(2)}(0)+2d^2\chi_{xz}^{(2)}(0)] \ . \end{aligned} \tag{78}$$

The corresponding eigenvalues of Eq. (77) in the general case turn out to be

$$\begin{aligned} \kappa_{1,2}=1-\frac{J^2}{2}&\{\chi_L^{(2)}(0)+\chi_T^{(2)}(0)+\chi_{xy}^{(2)}(0)+d^2[\chi_T^{(2)}(0)+\chi_{xy}^{(2)}(0)+4\chi_{xz}^{(2)}(0)]\} \\ \mp\frac{J^2}{2}&(\{\chi_T^{(2)}(0)-\chi_L^{(2)}(0)+\chi_{xy}^{(2)}(0)+d^2[\chi_T^{(2)}(0)+\chi_{xy}^{(2)}(0)]\}^2 \\ &+8\{\chi_{xz}^{(2)}(0)+d^2[\chi_L^{(2)}(0)+\chi_{xz}^{(2)}(0)]\}\{\chi_{xz}^{(2)}(0)+d^2[\chi_T^{(2)}(0)+\chi_{xy}^{(2)}(0)]\})^{1/2} \ , \end{aligned} \tag{79}$$

where the eigenvalue $\kappa_1(d,h,T)$ stands for the upper and $\kappa_2(d,h,T)$ for the lower critical line, respectively.

For zero anisotropy and an applied magnetic field h, one has

$$\chi_{\mu\nu}^{(2)}(0)=\chi^{(2)}(0)\delta_{\mu\nu}$$

and from Eqs. (78) and (79) one obtains

$$\begin{aligned} \kappa_1&=1-J^2\chi_T^{(2)}(0) \ , \\ \kappa_2&=1-J^2\chi_L^{(2)}(0) \ , \end{aligned} \tag{80}$$

for the pure quantum Heisenberg spin-glass model. Here, the vanishing of the degenerate eigenvalue κ_1 determines the upper critical line [the so-called Gabay-Toulouse (GT) line[32]] which describes the transition from the ergodic to the nonergodic spin-glass phase. Note that, in this case, the upper critical line can be determined by the equivalent condition of vanishing of the transverse component of the spin-glass order parameter ($q_T=0$). The lower critical line [the so-called Almeida-Thouless (AT) line[33]] resulting from the condition $\kappa_2=0$ describes, in turn, the transition in the field-temperature plane from a region with small nonergodicity to strong nonergodicity (and cannot be determined from the corresponding condition $q_L=0$ due to the applied field which makes q_L nonzero everywhere). Moreover, since the lower critical line already lies in the spin-glass region, its exact calculation would presumably require the quantum analog of the Parisi replica symmetry-breaking scheme.[34] However, explicit calculations of the static properties in this region of the h-T phase diagram would be extremely complicated even for the simplest assumption concerning the replica-breaking scheme.

In the case of zero magnetic field $h=0$, but nonzero anisotropy d, one has

$$\chi_L^{(2)}(0)=\chi_T^{(2)}(0)=\chi^{(2)}(0)$$

and $\chi_{xy}^{(2)}(0)=\chi_{xz}^{(2)}(0)$, which, subsequently results in

$$\begin{aligned} \kappa_1&=1-J^2[\chi^{(2)}(0)+2\chi_{xy}^{(2)}(0)](1+2d^2) \ , \\ \kappa_2&=1-J^2[\chi^{(2)}(0)-\chi_{xy}^{(2)}(0)](1-d^2) \end{aligned} \tag{81}$$

with the eigenvalue κ_1 being nondegenerate and κ_2 being twofold degenerate. In the absence of the anisotropy ($d=0$) the above eigenvalues vanish at the same critical temperature T_c [Eq. (41)], i.e., the lower and upper critical lines coincide in zero field. For finite anisotropy, this is no longer true and the corresponding phase diagram is presented in Figs. 5 and 6 for different values of the quantum spin.

For finite anisotropy ($d\neq 0$) and the applied field ($h\neq 0$), the degeneracies of the eigenvalues κ_1 and κ_2 interchange with κ_1 being nondegenerate, as compared to the corresponding zero anisotropy case. Therefore, one expects a crossover behavior from the Heisenberg GT-type to Ising AT-like with increasing anisotropy (or from Ising-type to Heisenberg-type for a given anisotropy d and increasing magnetic field h), as can been seen in the field-temperature (h-T) phase diagrams calculated (Figs. 7 and 8) numerically for several values of the anisotropy constant d. Here, for the rather narrow interval of anisotropies, one observes the characteristic changeover from

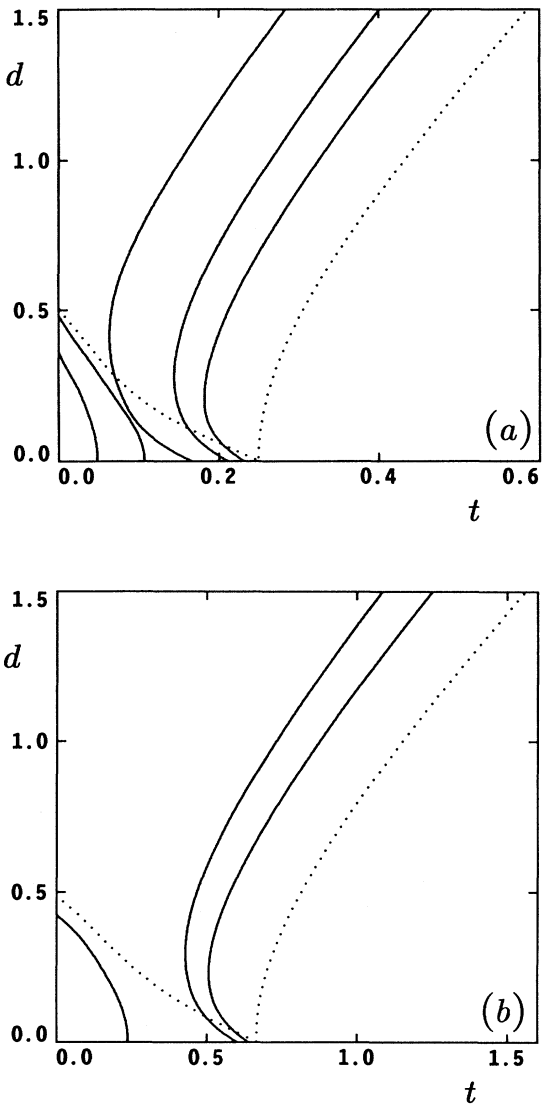

FIG. 5. The anisotropy-temperature ($t=k_BT/J$) phase diagram for (a) $S=\frac{1}{2}$, (b) $S=1$ ($\kappa_1=0$ and $\kappa_2=0$ for upper and lower critical lines); zero-field case (dotted lines), (a): $h/J=0.125$, 0.25, 0.5, (b): $h/J=0$, 0.25, 0.5 (solid lines, from right to the left, respectively; the lower critical line for $h=0.5$ is suppressed).

the convex-type AT line to the concave shape of the critical line typical for GT behavior. Moreover, this crossover manifests itself in the anisotropy-temperature phase diagram ($d-T$) (Figs. 5 and 6) as a characteristic reentrant behavior at the upper critical line for nonzero h. Note, however, that in the nonzero field case, the upper GT line cannot be determined from the condition $q_T=0$. The remarkable feature of the random DM anisotropy is that it leads to a mixing of the longitudinal and transverse modes and for $h\neq 0$ one has $q_L\neq 0$ as well as $q_T\neq 0$ everywhere. Therefore, the determination of the phase diagrams and critical lines can only follow via the full stability analysis [Eqs. (72)–(79)].

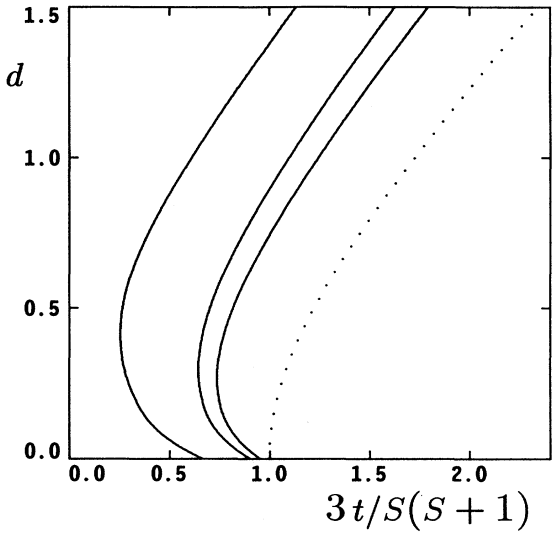

FIG. 6. The anisotropy-temperature ($t=k_BT/J$) phase diagram (upper critical lines $\kappa_1=0$) for $h=0$ (dotted line) and $h=0.5$ (solid lines) and for different values of the quantum-spin number: $S=\frac{1}{2}$, 1, $\frac{3}{2}$ (from the left to the right, respectively).

VI. SUMMARY AND DISCUSSION

We have considered the effect of the random Dzyaloshinsky-Moriya interactions in Heisenberg quantum spin glasses using the thermofield dynamics as a substitute for the n-replica trick. As far as critical (i.e., instability) lines are concerned, the presence of random DM anisotropy leads to a crossover at the upper critical line from the Ising [$T_c(h)\propto h^{2/3}$] to the Heisenberg behavior [$T_c(h)\propto h^2$] manifested on the field-temperature (h-T) phase diagram with increasing field. The lower critical line, in turn, exhibits the reversed behavior, i.e., the crossover from Heisenberg-like to typical AT Ising behavior. However, our numerical calculations show that this characteristic effect is rather weak and occurs for small anisotropies d. For larger values of the anisotropy constant ($d>0.3$), the upper critical line is practically indistinguishable from the shape of the AT line while the lower critical line is suppressed for $d>0.5$. This might suggest that random DM interaction is responsible for the lack of the characteristic GT-like shape of the upper critical line, as has been detected in many experiments with Heisenberg spin glasses. Therefore, the actual observation of the crossover phenomenon would presumably require samples with precise controlled doping since the addition of a few hundred parts per million of nonmagnetic impurities increase the DM anisotropy by orders of magnitude,[12] thus affecting the picture (in the field-temperature critical line) considerably. However, it is interesting to note that measurements on *Cu*Mn alloys doped with Au impurities (which induce strong DM anisotropy) indeed show that the irreversibility onset line progressively changes from GT-like to AT-like as the concentration of Au is increased[35] in consistency with the

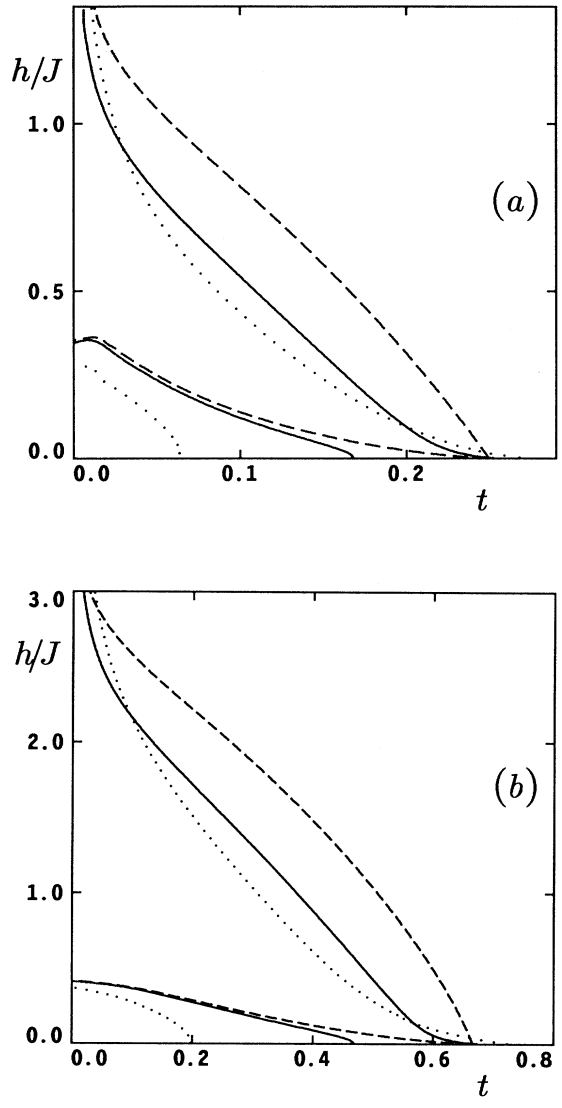

FIG. 7. The field-temperature ($t=k_BT/J$) instability lines (upper and lower) for (a) $S=\frac{1}{2}$, (b) $S=1$, and various anisotropies including $d=0$ (dashed lines), $d=0.1$ (solid lines), and $d=0.3$ (dotted lines). The $d=0.1$ critical lines show Ising-to-Heisenberg crossover (upper line) and reversed behavior (lower line).

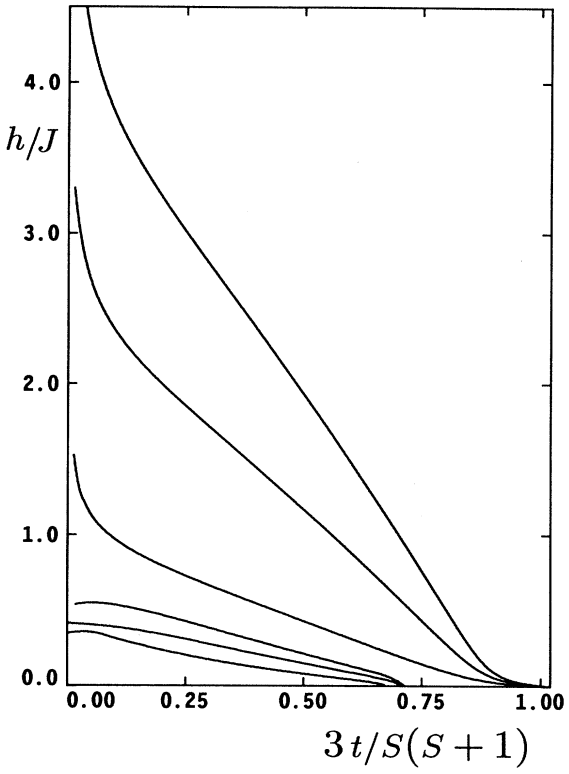

FIG. 8. The field-temperature ($t=k_BT/J$) instability lines (upper and lower) for fixed anisotropy $d=0.1$ and different quantum-spin numbers: $S=\frac{1}{2}$, 1, $\frac{3}{2}$ (from bottom to the top for lower and upper instability lines, respectively).

presented picture of random DM anisotropy.

Another characteristic feature of the random DM interaction is a strong mixing of the longitudinal and transverse modes. In our calculations this is best seen from the field and temperature dependence of the longitudinal and transverse susceptibilities. Specifically, the presence of DM anisotropy is reflected by a rather weak temperature dependence of various susceptibilities (a plateau for strong anisotropies) in the spin-glass phase as compared to the pure Heisenberg spin-glass case. Moreover, the calculations which include the effect of magnetic field indicate the pronounced similarity of the shape for longitudinal and transverse susceptibilities as a function of temperature. For example, the cusp of the transverse susceptibility with field, present in the pure case as well as in the case of Heisenberg spin glass with nonrandom uniaxial anisotropy,[12] is washed out in the DM case as a result of mixing of various modes.

In closing, we would like to stress that, although we have considered here a specific case of random anisotropy, it would be interesting to check whether a similar picture persists in other cases which may be present in real spin-glass systems. Of special interest are anisotropies which randomly mix spin directions, e.g., random dipole-dipole interaction[36] or even random local anisotropies as uniaxial anisotropy with random axial directions.[37]

ACKNOWLEDGMENTS

The authors are grateful to Professor Klaus D. Usadel for many stimulating discussions and critical reading of the manuscript. This work was supported by the Sonderforschungsbereich 166: "Strukturelle und magnetische Phasenübergänge in Übergangsmetall-Legierungen und Verbindungen."

*Permanent address: Institute for Low Temperature and Structure Research, Polish Academy of Sciences, P. O. Box 937, 50-950 Wroclaw 2, Poland.

[1]H. Albrecht, E. F. Wassermann, F. T. Hedgcock, and P. Monod, Phys. Rev. Lett. **48**, 819 (1982).
[2]A. Fert, P. Pureur, F. Hippert, K. Baberschke, and F. Bruss, Phys. Rev. B **26**, 5300 (1982).
[3]S. Murayama, K. Yokosawa, Y. Miyako, and E. F. Wassermann, Phys. Rev. Lett. **57**, 1785 (1986).
[4]D. M. Cragg and D. Sherrington, Phys. Rev. Lett. **16**, 1190 (1982).
[5]S. A. Roberts and A. J. Bray, J. Phys. C **15**, L527 (1982).
[6]D. J. Elderfield and D. Sherrington, J. Phys. A **15**, L437 (1982); J. Phys. C **16**, 4865 (1983).
[7]H.-J. Sommers and K. D. Usadel, Z. Phys. B **47**, 63 (1982).
[8]K. D. Usadel, K. Bien, and H.-J. Sommers, Phys. Rev. B **27**, 6957 (1983).
[9]G. Brieskorn and K. D. Usadel, J. Phys. C **19**, 3413 (1986).
[10]T. K. Kopeć, G. Büttner, and K. D. Usadel, Phys. Rev. B **41**, 9221 (1990).
[11]G. Büttner and K. D. Usadel, Europhys. Lett. **14**, 165 (1991).
[12]P. M. Levy and A. Fert, Phys. Rev. B **23**, 4667 (1981).
[13]S. Schultz, E. M. Gullikson, D. R. Fredkin, and M. Towar, Phys. Rev. Lett. **45**, 1508 (1980); J. Owen, M. E. Brown, V. Arp,and A. Kip, J. Phys. Chem. Solids **2**, 85 (1957).
[14]I. Dzyaloshinsky, J. Phys. Chem. Solids **4**, 241 (1958); T. Moriya, Phys. Rev. Lett. **4**, 5 (1960).
[15]L. R. Walker and L. W. Walstedt, Phys. Rev. Lett. **47**, 1624 (1981); J. Magn. Magn. Mater. **31-34**, 1289 (1983).
[16]G. Kotliar and H. Sompolinsky, Phys. Rev. Lett. **53**, 1751 (1984).
[17]P. M. Goldbart, J. Phys. C **18**, 2183 (1985).
[18]K. H. Fischer, Z. Phys. B **60**, 151 (1985).
[19]A. J. Bray and M. A. Moore, J. Phys. C **13**, L419 (1980).
[20]H.-J. Sommers, J. Magn. Magn. Mater. **22**, 267 (1981).
[21]T. Yamamoto and H. Ishii, J. Phys. C **18**, 6225 (1985); H. Ishii and T. Yamamoto, *ibid.* **20**, 6053 (1987).
[22]K. D. Usadel, Solid State Commun. **58**, 629 (1986); K. D. Usadel and B. Schmitz, *ibid.* **64**, 975 (1987); K. D. Usadel, Nucl. Phys. B **5A**, 91 (1988).
[23]V. Dobrosavljević and R. Stratt, Phys. Rev. B **36**, 8484 (1987).
[24]T. K. Kopeć, J. Phys. C **21**, 297 (1988); **21**, 6053 (1988).
[25]T. K. Kopeć, K. D. Usadel, and G. Büttner, Phys. Rev. B **39**, 12 418 (1989). G. Büttner and K. D. Usadel, *ibid.* **41**, 428 (1990).
[26]H. Umezawa, Y. Takahashi, and H. Matsumoto, *Thermo Field Dynamics and Condensed States* (North-Holland, Amsterdam, 1982).
[27]P. C. Martin, E. Siggia, and H. Rose, Phys. Rev. A **8**, 423 (1973).
[28]H. Sompolinsky and A. Zippelius, Phys. Rev. Lett. **47**, 359 (1981).
[29]H. Matsumoto, Y. Nakano, and H. Umezawa, J. Math. Phys. **25**, 3076 (1984).
[30]D. Sherrington and S. Kirkpatrick, Phys. Rev. Lett. **32**, 1972 (1975).
[31]S. F. Edwards and P. W. Anderson, J. Phys. F **5**, 965 (1975).
[32]M. Gabay and G. Toulouse, Phys. Rev. Lett. **47**, 201 (1981).
[33]J. R. L. De Almeida and D. J. Thouless, J. Phys. A **11**, 983 (1978); D. M. Cragg, D. Sherrington, and M. Gabay, Phys. Rev. Lett. **49**, 158 (1982).
[34]G. Büttner and K. D. Usadel, Phys. Rev. B **42**, 6385 (1990).
[35]N. de Courtenay, A. Fert, and I. A. Campbell, Phys. Rev. B **30**, 6791 (1984).
[36]A. J. Bray and M. A. Moore, J. Phys. C **15**, 3897 (1982).
[37]K.-H. Fischer and A. Zippelius, J. Phys. C **18**, L1138 (1985).